



Mitigating liquefaction risks for buildings on circular footings: a numerical modeling approach

Manendra Singh¹ · Siddhant Singh² · Rahul Shakya¹

Received: 26 July 2023 / Accepted: 9 August 2024 / Published online: 30 August 2024
© Springer Nature Switzerland AG 2024

Abstract

Liquefaction occurs when loose saturated sand loses its strength as a result of dynamic loading and begins to behave like a viscous fluid rather than a solid. This causes a huge reduction in effective stress, leading to loss of lives and property due to structure tilting, collapse, and foundation settlement. The 2001 Bhuj Earthquake triggered liquefaction in some areas of Gujarat and damaged buildings, bridges, ports, and dams. This study examines the behaviour of Kandla port's shallow foundation due to liquefiable soil during the 2001 Bhuj earthquake using finite element method by PLAXIS 3D software. Static and dynamic analyses of building founded on circular footing in terms of settlement, effective stress, and excess pore water pressure have been carried out. Also, vertical drain's liquefaction mitigation capability was investigated in this study. In the presence of buildings, vertical and horizontal deformation at the ground's surface and below the foundation were observed to be highest via dynamic analysis, with vertical deformation being smaller than horizontal deformation. This research revealed that dynamic settlements are higher than static settlement and, the vertical drains reduce excess pore water pressure and enhance effective stress. Dynamic analysis reveals that in the presence of buildings, vertical and horizontal deformation peaks at the ground's surface and beneath foundations, with vertical deformation smaller than horizontal. This study comprehensively explores earthquake-induced hazards, factors influencing liquefaction, and their impact on buildings. By examining the mechanisms through which earthquakes trigger hazards and liquefaction in structures, the research aims to enhance our ability to mitigate damage effectively.

Keywords Liquefaction · Circular foundation · FEM · Dynamic analysis · UBC 3D-PLM

Introduction

Some of the most spectacular examples of earthquake damage have occurred when soil deposits have lost their strength and appeared to flow as fluids. In this phenomenon, termed liquefaction, the strength of the soil is reduced, often drastically, to the point where it is unable to support structures or remain stable [24]. In undrained conditions, seismic loading

surges Excess Pore Pressure (EPP), reducing soil's effective stress, thus soil acts as a viscous fluid and effective stress becomes zero [38]. First documented liquefaction impact was Libson Earthquake of November 1755. The 1964 Niigata and Alaska earthquakes wrecked lives and property, including buildings. A 7.7-magnitude (on Richter scale) earthquake hit Gujarat's Bhuj area, killing thousands of people and destroying houses, bridges, roads, and ports. Liquefaction in Rann of Kachchh's sandy soil caused huge devastation. Land instability, known as Lateral Spreading, caused massive harm. The scientific community acknowledged additional research is required to mitigate the probability of liquefaction-induced hazards in liquefaction-prone locations to assure the safety of buildings and infrastructure. Rollins and Seed [32] studied the influence of liquefaction on the building. Their study and references from various case histories, centrifuge tests, and shake table test data concluded that excess pore pressure near the building is much lower than free field conditions for the same depth. Study

✉ Rahul Shakya
rshakya@nith.ac.in

Manendra Singh
manendra@nith.ac.in

Siddhant Singh
Sid.singh997@gmail.com

¹ Department of Civil Engineering, National Institute of Technology, Hamirpur, Himachal Pradesh 177005, India

² OST Slope Protection Engineering India Pvt. Ltd., Gurgaon, Haryana, India

revealed that the excess pore pressure generation for area having loose sand is more than the free field for the same depth. Also, the study concluded that the soil having initial static stress due to the building has greater liquefaction resistance for dense sand and less resistance for loose sand. Yasui [42] analysed the effect of 1990 earthquake in the Philippines in which RCC building in Dagupan city was destroyed due to liquefaction. Settlement and inclination of building have also been studied. It was concluded that the settlement and tilting angle of the structure decreased with increase in area and the width of the building. Liu and Dobry [26] have studied the seismic response of shallow foundations on the sand susceptible to liquefaction. Eight centrifugal model experiments have been conducted to investigate the settlement of the shallow foundation and the effect of soil densification on bearing capacity and settlement of shallow foundation. When the soil was not compacted, the soil became more impervious, and negative excess pore pressure developed which increased the post-liquefaction settlement. Rollins et al. [33] studied the performance of vertical drains to mitigate liquefaction. For research work, prefabricated vertical drains were installed at the Barnard Elementary School Library in San Diego, California. Detonating blast method was used to simulate an earthquake. It was seen that the vertical drains effectively increased the rate of dissipation of EPP. Also, the installation process of vertical drains densifies the soil around the drain which may have increased liquefaction resistance. Wakamatsu and Numata [41] analysed the effect of liquefaction on building damage during the Kobe earthquake of 1995. Study includes soil data from 165 affected and non-affected buildings during Kobe earthquake. They had taken references from various research papers and introduced the term Liquefaction Potential Index (PL), which was correlated with the severity of the ground motion effect. It was also concluded that when there is an increase in the liquefaction susceptibility, then there is a decrease in the rate of damage in building irrespective of ground shaking intensity because of the absorbing nature and non-linear property of soil. The Waheed and Asmael [28] used FEM by PLAXIS 3D software to study how shallow foundations behave during liquefaction. The results showed that the Mohr–Coulomb model overestimates foundation settlement, while the soft soil model underestimates it. The experiment was based on the model of Dashti et al. [9]. He also studied the effect of the adjacent building on the model. It was found out that the taller building with a heavier shallow foundation settles more than a smaller building with a lighter shallow foundation due to liquefaction. Marques et al. [29] used a dynamic centrifuge experiment to explore liquefaction on shallow foundations. The structure had greater settlement than the free field. Post-earthquake loading would cause footing liquefaction. Foundation and free field post-liquefaction settlements were similar. Maximum

foundation settlement occurs under earthquake stress, and excess pore pressure dissipates to free-field levels. The building's swaying caused more vertical acceleration than vertical input acceleration. Rajarathnam et al. [34] conducted SPT test of 666 number of boreholes across Chennai city and prepared the liquefaction hazard map of Chennai. The significant findings of their research were that the severity of liquefaction in any area has direct relation with the thickness of the liquefiable layer and is inversely proportional to the layer's distance in the downward direction to the ground surface. The area that was more prone to liquefaction had a very low value of N_{60} and a higher depth of water table. Deep foundations often fail in buckling and are affected due to liquefaction. Connor Patric Hayden [16] conducted a test on the building and soil model and found out that settlement in the structure occurs mainly during strong shaking. If the structure is founded on a shallow foundation the value of the deformation was greater than that during free field condition. The higher value of relative density tends to result in less settlement. Abdullah et al. [3] utilised PLAXIS 2D to model tyre chips with vertical and horizontal framing underneath a shallow foundation for the 1995 Hyogo-Ken earthquake. Tyre chips minimise vertical displacement, study finds. Chips reduce vertical ground motion. Ayoubi and Pak [4] analysed the settling of a shallow foundation owing to liquefaction using shaking table test. Denser soil layers may limit settling by 50% compared to loose soil layers. Dense layers reduce settlement linearly. The interface between thick and loose soils had the most settlement. PGA and contact pressure are directly related to settling. Onur et al. [31] used FEM using PLAXIS 2D software to study seismic motion on a raft-founded building in Eskisehir, Turkey. Soil for the study was taken as silty sand and loose sand. On the other hand, the HS soil model gives more accurate results when simulating soil that can be liquefied. Efforts to mitigate liquefaction by accelerating the rate of water flow can be carried out such as the use of vertical drainage. Previously (Seed and Booker [35]) stated that the use of gravel drainage can provide an efficient method to prevent the development of pore water pressures that are too high and the distance between vertical channels can be made less than the distance required for water to flow vertically to the free surface. A comparison study has been done on the effectiveness of horizontal drainage in different geometric layouts [10]. The study in [13] has analyzed the performance of vertical drainage under the building together with the dynamic response of the foundation shown by the dissipation behavior of soil excess pore pressure. Experimental measurements as well as numerical simulations were carried out to describe the increase in excess pore pressure to liquefaction [6]. García-Torres and Madabhushi [13] observed that vertical drains decrease EPP which may reduce the possibility of liquefaction phenomenon. The viability of vertical

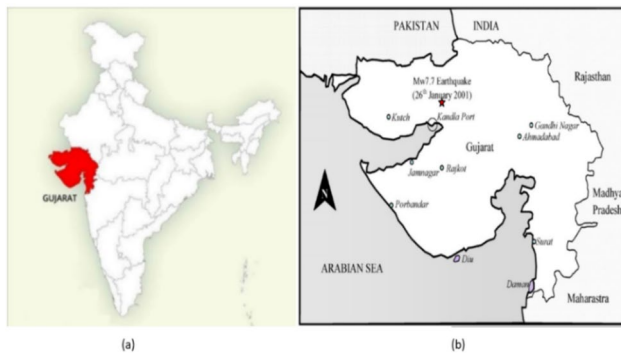


Fig. 1 Location of site considered for the study [8]

drains and their placement below the foundation were studied using a dynamic centrifuge model test. The drain was built with rubble bricks for enhanced permeability, minimising liquefaction pressure. According to the research, drains lower excess soil pore pressure and speed up its dispersion and increases effective stress. Vertical drains operate as soil shear reinforcements, minimising lateral spreading during liquefaction. The liquefaction also affects the underground tunnel’s seismic response [40] and tunnel’s damage depends upon the level of water table, if water table rises to the level of the crown of the tunnels. Forcellini [11] investigates the role of the water level on a typical Italian building during the 23 November 1980 Irpinian–Basilicata earthquake by performing several 3D numerical models of the entire system (soil–foundation–structure). The results show that the shear mechanisms and the consequent permanent deformations inside the soil are driven by the presence of the water. Therefore, knowing the position of the water level (and eventually how it changes during the seasons) is fundamental in order to assess the seismic vulnerability of structural configurations. Singh and Maheshwari [36] conducted an analytical study to determine the effect of liquefaction on strip footings resting on sand. Liquefaction induced settlement is directly depends upon the peak ground acceleration. The



Fig. 2 Layered strata of Kandla Port Soil

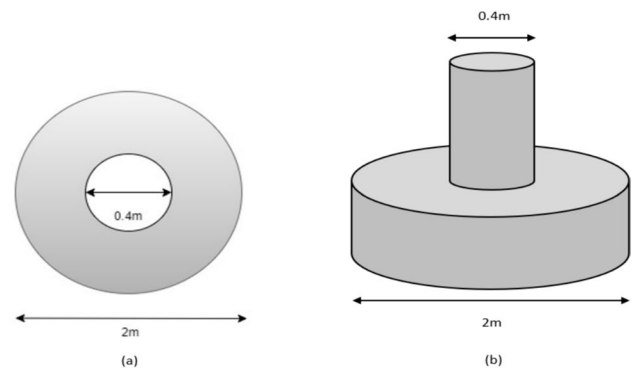


Fig. 3 Line diagram of footing considered for the study

study done by Li and Li [25] focuses on the test error of single dynamic characteristics, analyzing the impact of experimental errors on peak ground acceleration. The study done by Hanindya et al. [14] emphasized the importance of analyzing liquefaction potential based on earthquake wave propagation from bedrock to the ground surface. Harianto et al. [15] determine the effect of timber pile addition on soil settlement and the increase in bearing capacity and concluded that Eucalyptus Pellita timber piles can be used as an alternative to handle sandy soils in areas prone to liquefaction, showing a reduction in settlement by 18% in preloading tests and 68% in seismic load tests. The research emphasized the importance of further studies to improve the reinforcement of timber piles, including testing different installation patterns and relative densities for better performance. Forcellini [12] proposed a framework to assess the SSI effects with an equivalent fixed-based model that considers the SSI effects by applying the period of elongation and the damping increase. This study comprehensively explores earthquake-induced hazards, factors influencing liquefaction, and their impact on buildings. By examining the mechanisms through which earthquakes trigger hazards and liquefaction in structures, the research aims to enhance our ability to mitigate damage effectively. Emphasizing the critical role of strategically positioning vertical drains to mitigate liquefaction risks, the study underscores the necessity for ongoing research efforts grounded in both empirical findings and a nuanced understanding of soil water pressure dynamics. By prioritizing the development of prevention strategies, particularly through optimal vertical drain placement, and advancing our understanding of soil mechanics, the research seeks to minimize the adverse effects of earthquake hazards and liquefaction on infrastructure. Despite extensive studies on seismic performance, there remains a notable gap in research on liquefaction mitigation methods, necessitating further exploration of alternatives such as prefabricated drains, stone columns, and sand drains. The result of this study was compared with the experimental study done by

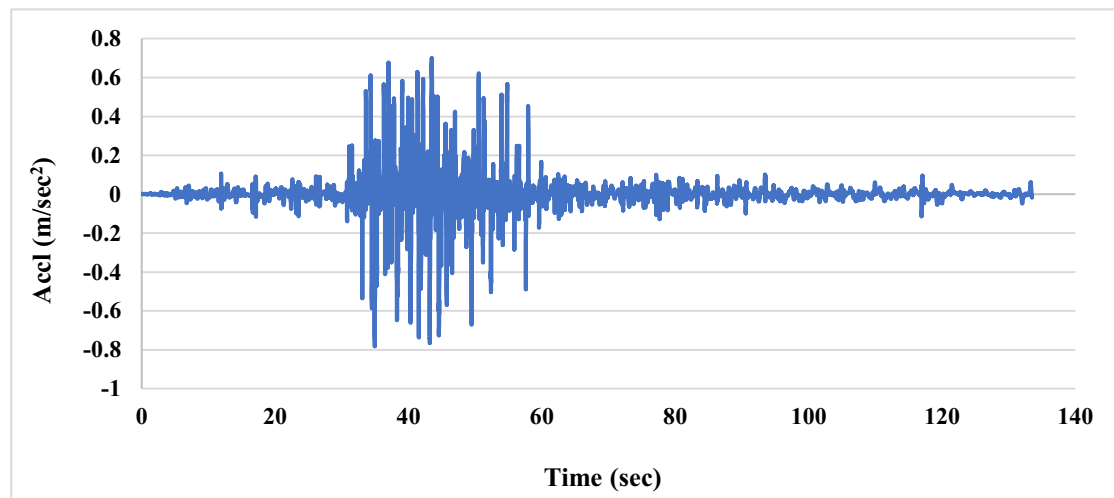


Fig. 4 Acc. versus time plot for Bhuj Earthquake

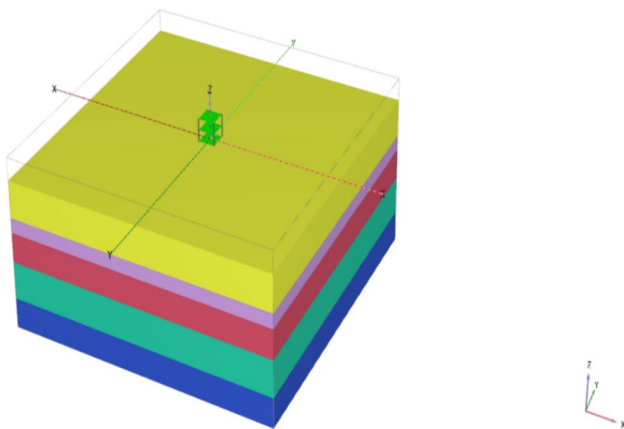


Fig. 5 Soil building model in Plaxis 3D

Bray et al. [7]. They conducted a dynamic centrifuge test on the liquefiable sand layer of Nevada. The result from their test was taken as a reference for the current research work. Bray and his research team aimed to determine the settlement of shallow foundations because of liquefaction and to safeguard the structures from these types of hazards.

Problem description

The location of Kandla Port, located in the coastal Kachchh district of Gujarat state in western India, has been selected for investigation in this research. Being a coastal region, the groundwater table is high and the soil deposit is completely saturated. According to India's seismic zone map, this location falls under zone V.

The primary objective of this research is to investigate the behaviour of a structure with a shallow circular base at Kandla Port, Kutch soil deposit, during the liquefaction condition caused by the Bhuj earthquake of 2001. In this research, shallow circular footings with a 1 m radius were evaluated to withstand the load of three-story structures with a 3 m × 3 m size.

Site selection

Kandla is a city in Gujarat located on the western shore of the Arabian Sea. This place is on the Rann of Kachchh's south-eastern shore. This is one of Gujarat's main seaports, which was significantly devastated by the Bhuj Earthquake. The epicentre of the earthquake was around 9 km southwest in Bhachau of Kutch district of Gujarat. The epicentre of earthquake was about 50 km from the Kandla port. Figure 1 shows the site location on the map.

Soil properties

The soil profile at Kandla Port was composed of unconsolidated clays, silts, and sands, according to a study by Dash et al. [8]. When a powerful earthquake struck the area, it was evident that the rigidity of the clay layer would diminish and that the sand layer would be prone to liquefaction. Sitharam and Govindaraju [37] concluded that the degradation of the clay layer's stiffness is a function of the Plasticity Limit also provided that the Atterberg Limits for the sand layer, which were relatively close to those provided by Dash et al. [8]. Figure 2 depicts the layered strata of Kandla Port Soil. The soil parameters provided by Dash et al. [8] have been utilized for the current study. The GWT in the area fluctuates from 1.2 m and 3 m below

the ground. For this investigation, GWT was assumed to be 2.5 m below ground level.

Selection of foundation

There is less concrete volume and reinforcing needed for circular foundations than there is for square foundations when the foundation footings are equal in width or diameter, according to Oladayo O Komolafe et al., [23]. Numerous modern infrastructure projects, such as bridges, water storage tanks, and residential homes, are built on circular foundations. So, a circular foundation with a diameter of 1 m was chosen for this research. Figure 2 depicts the footing diagram used in this study. The diameter of the column was taken as 0.4 m, as shown in Fig. 3.

Earthquake ground motion

India has a high frequency of earthquakes. About more than 50% area of the country is prone to earthquakes.

The Bureau of Indian Standards modified the India earthquake seismic zonation map in 2002 after the 2001 Bhuj earthquake. According to the new mapping, Gujarat comes under Zone V of the seismic zonation map. Gujarat Earthquake (2001) was 3rd largest and the 2nd most destructive earthquake that occurred in India. This was one of the most catastrophic earthquakes that hit India, when the country was celebrating its 52nd Republic Day on 26-Jan-2001 at 8:46 AM IST, in the western coastal part of the country. The magnitude recorded was 7.7 M_w at 23.36°N Latitude and 70.34°E longitude at a depth of 23.6 km below ground. It left nearly millions of people affected and about 20,000 people lost their lives. This earthquake is named as Bhuj Earthquake as this was one of the most severally affected flooded areas, was used in this study for the analysis. Three parameters which significantly affect the liquefaction potential of soil are Peak ground acceleration (PGA), Frequency and Duration of earthquake. However, the magnitude of the Bhuj earthquake is not as high but its duration is too large that caused significantly damage in Bhuj and Kutch regions. Figure 4 depicts the seismic

Table 1 Mohr–Coulomb material model for soil layer

Parameters	Soil layers				
	Soft clay	Fine sand	Coarse sand	Hard clay	Clayey sand
Depth (m)	0–10	10–14	14–22	22–32	32–40
Dry unit weight γ_d (kN/m ³)	16	17	17	18	18
Saturated unit weight γ_{sat} (kN/m ³)	18	19.5	19.5	20.4	19.8
modulus of elasticity E (kN/m ³)	4800	4200	4800	19200	10800
Poisson’s ratio μ	0.3	0.3	0.3	0.3	0.3
c (kN/m ³)	10	0	0	100	0
friction angle (ϕ^o)	0	29	30	0	35
Dilatancy angle (φ^o)	0	0	0	0	5

Table 2 UBC 3D-PLM material model for sand layer

Parameters	Fine sand	Coarse sand
Drainage Condition	Undrained (A)	Undrained (A)
Peak Friction Angle (φ_p^o)	30.3	31.3
Friction angle at constant volume (φ_{cv}^o)	29	30
Effective cohesion (c')	0	0
Elastic Bulk Modulus (k_B^e)	713.73	675.105
Elastic Shear Modulus (k_G^e)	1019.61	964.436
Plastic Bulk Modulus (k_G^p)	616.94	350.09
Power for stress dependency of k_G^e (n_e)	0.5	0.5
Power of stress dependency of k_B^e (m_e)	0.5	0.5
Power of stress dependency of k_G^p (n_p)	0.4	0.4
Failure Ratio (R_f)	0.7486	0.7676
Reference Stress P_A (kN/m ³)	100	100
Parameter for adjusting densification (fac_{dens})	1	1
Parameter for adjusting post-liquefaction (fac_{post})	1	1
Corrected SPT No. (N_1) ₆₀	13	11

time history of the Bhuj 2001 earthquake, which was taken from bedrock level and applied at the base of the model.

Numerical modelling

In this research, the FEM based PLAXIS 3D software was used to examine the influence of liquefaction on buildings founded on circular footings. After performing a sensitivity analysis, a model size of 50 m × 50 m × 40 m in the x, y and z direction has been used in this study.

Soil and building modelling

The geometry of the soil domain was determined using the methodology of trial and error. In the context of this, the most suitable soil range for this investigation was 50 m × 50 m × 40 m as shown in Fig. 5. To perform the finite element computation, the model was discretized into smaller finite number of 10-noded tetrahedral elements. The meshing of the domain is carried out based on the fully automatic generation of finite elements inherent to the PLAXIS 3D program. Five basic meshing schemes are available (very coarse, coarse, medium, fine, and very fine mesh), while allowing the user for further refinements of a region, around a line or around a node. A very coarse mesh fails to capture the important characteristic responses of the domain. Beyond optimally fine meshes, there are chances of the accumulation of numerical errors, thereby producing inaccuracy in the obtained information. Moreover, very fine meshing is also affected by excessive computation time. Hence, a convergence study has been adopted to determine the optimum mesh configuration for the simulation of model. When modelling the soil domain, tetrahedral elements with 10 nodes and an average size of 1.66 m were considered.

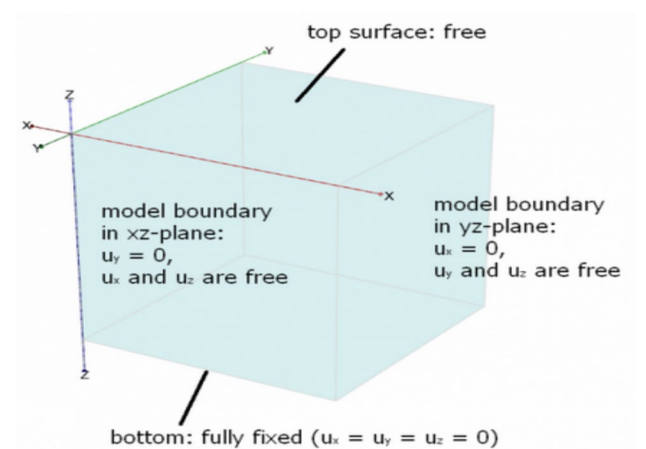


Fig. 6 Boundary condition for static analysis

Lysmer and Kuhlemeyer [27] suggest that for optimal performance, a mesh's average element size should be smaller than or equal to one-eighth of the wavelength of the highest-frequency component of the input wave. (i.e. average element size $\leq \lambda/8$). In the present analysis, this criterion has been satisfied, and also the sensitivity analysis with different element sizes and reduced the element size to reach a stable result (i.e. 1.66 m), in which further reduction in element size gives the same result. A 6 m × 6 m, three-story structure was taken for this study as presented in Fig. 5. M25 grade of RCC was considered for the construction of buildings and foundations. The building's dead weight was about 780 kN and was distributed to the earth using four 1 m-diameter circular footings. Therefore, the load on individual footing was 195 kN.

For static analysis of each soil layer, the Mohr's-Coulomb material model was used for simulating the behaviour of stress strain relation. In numerical analysis UBC3D-PLM model [1] was used for simulating the behaviour of liquefaction susceptible soil. Liquefaction potential is defined by a

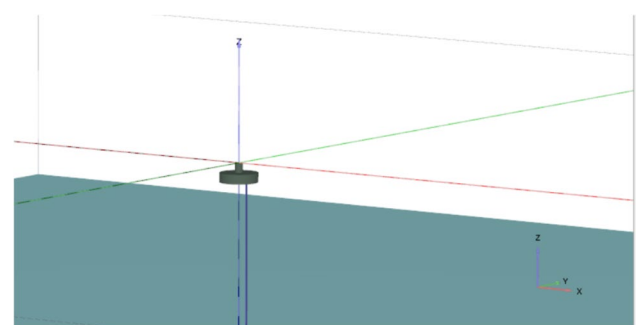


Fig. 7 Model analysed for determining bearing capacity

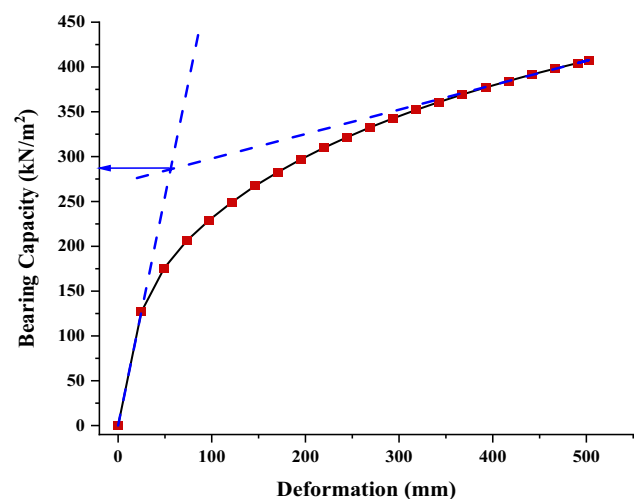


Fig. 8 Load-Settlement curve of circular footing for Kandla Port Soil below the foundation

Table 3 Horizontal and vertical settlements for both cases (case 1: foundation alone, case 2: foundation with structure) under dynamic loading

Settlement (mm)	Only the foundation experiences dynamic effects	Both the foundation and structure undergo loading
Vertical	3.686	13.375
Horizontal	0.726	2.790

parameter R_u (excess pore pressure ratio) in terms of mean effective stress (Eq. 1) and vertical effective stress (Eq. 2).

$$R_u = \frac{P'_i - P'_c}{P'_i} \tag{1}$$

where P'_i is the initial effective mean stress and P'_c is the current effective stress.

$$R_u = \frac{\sigma'_{vertical,i} - \sigma'_{vertical,c}}{\sigma'_{vertical,i}} \tag{2}$$

where $\sigma'_{vertical,i}$ is the initial vertical effective stress and $\sigma'_{vertical,c}$ is the current vertical effective stress.

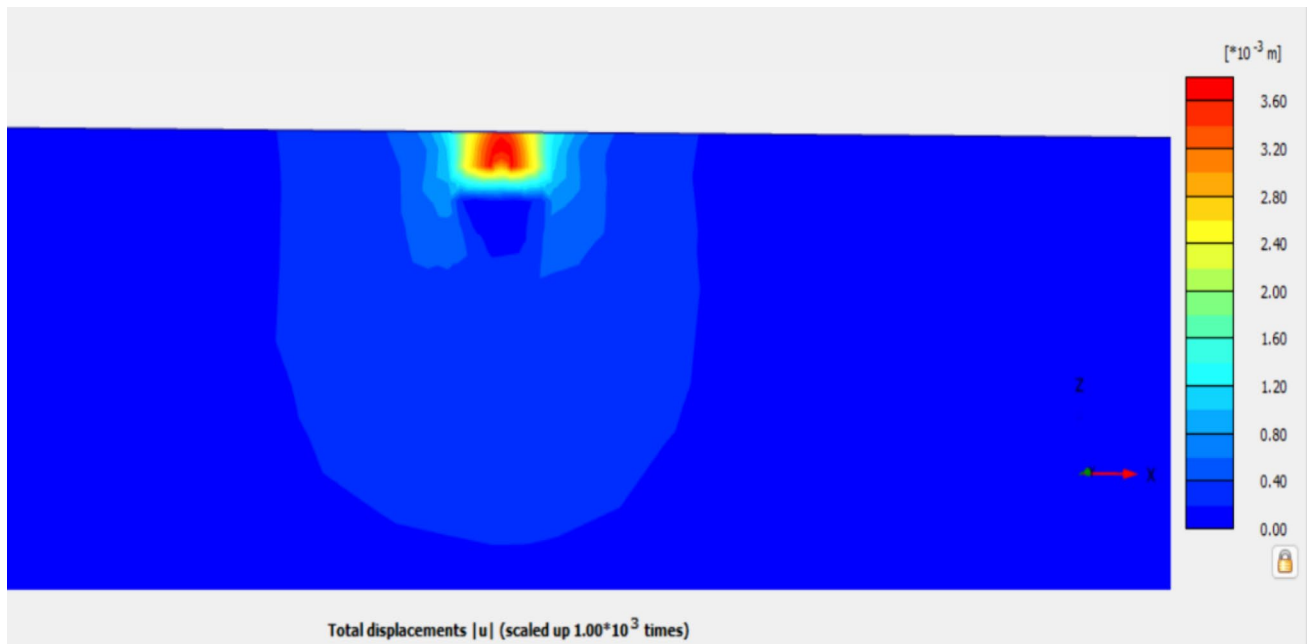


Fig. 9 Pressure bulb for case 1 (foundation alone) under dynamic loading

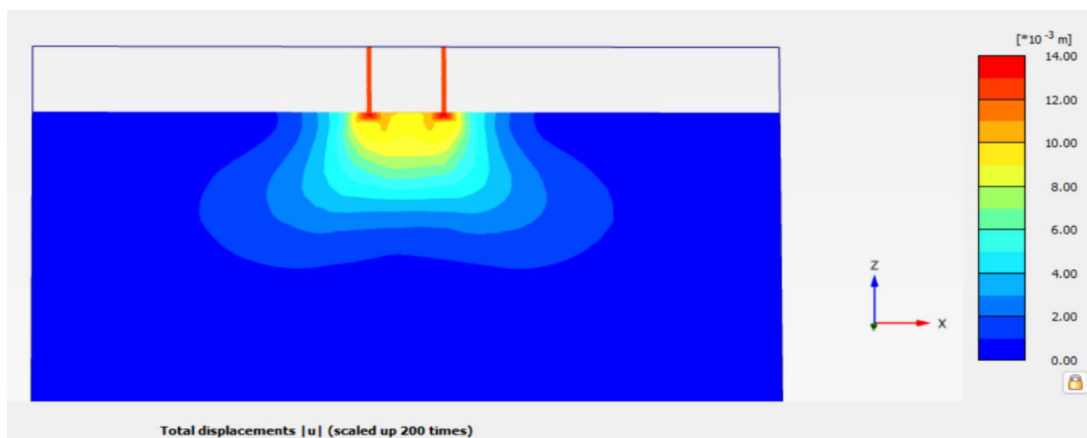


Fig. 10 Pressure bulb for case 2 (foundation with structure) under dynamic loading

If R_u is equal or greater than 1 then soil is prone to liquefy.

The Mohr's-Coulomb material model was chosen for modelling the behaviour of a non-liquefiable layer. Tables 1 and 2 exhibit the soil layer properties for the Mohr's-Coulomb model and the UBC 3D-PLM model, respectively.

Damping

While PLAXIS allows users to model dynamic loading and vibrations, it doesn't provide built-in features for simulating damping directly. Instead, it relies on users to input appropriate dynamic properties, including damping, based on the material properties and analysis requirements. In the present analysis, damping was incorporated through Rayleigh damping.

Rayleigh damping is a common approach to model damping in dynamic analysis. It involves a combination of mass-proportional damping and stiffness-proportional damping. Users can specify the damping ratios for both mass and stiffness terms based on the characteristics of the material

and the structure. Rayleigh damping is calculated using the following Eq. (3).

$$C = \alpha M + \beta K \tag{3}$$

where, M and K are mass and stiffness matrices and α and β are the Rayleigh damping coefficients, which are determined by using the Eq. 2.

$$\begin{Bmatrix} \alpha \\ \beta \end{Bmatrix} = \frac{2\zeta}{w_m + w_n} \begin{Bmatrix} w_m w_n \\ 1 \end{Bmatrix} \tag{4}$$

The damping ratio (ζ) characterizes the damping of vibrations, while the natural frequencies of the soil mass (ω_m and ω_n) correspond to the mode shapes labelled as 'm' and 'n'. It is important to note that the structure and soil mass exhibit distinct modes of vibration. In this context, the specific values chosen for 'm' and 'n' are 1 and 2, respectively, indicating that the soil-tunnel system is considered to vibrate exclusively in modes 1 and 2. Damping coefficients, α and β were determined for both RC liners and the surrounding soil using Eqs. 3 and 4. In this study damping ratio was selected as 10% and 2% for the soil and RCC respectively.

Boundary conditions

For static response, nodes along the XZ plane of the model were constrained in the Y-direction while remaining free to move in the X- and Z-directions. Similarly, nodes along the YZ-plane of the model were constrained in the X-direction while remaining free to move in the Y and Z-directions. Top surface freedom was maintained in all directions, while bottom boundary freedom was enforced in all directions as shown in Fig. 6. Lysmer and Kuhlmeyer [27] suggested a viscous absorbent boundary to represent the displacement condition in dynamic analysis, and this boundary was implemented in both the horizontal and vertical directions (XZ and YZ planes) for dynamic analysis. At the model's

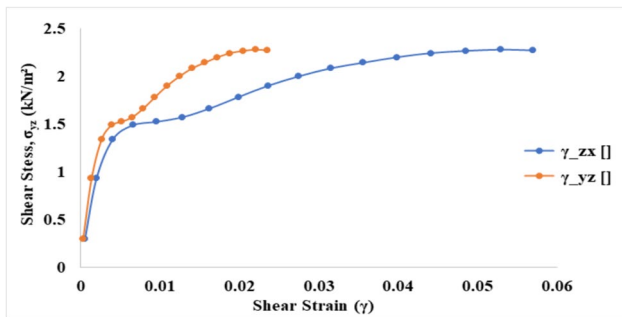


Fig. 11 Stress versus strain plot at centre of top layer for case 1 (foundation alone) under dynamic loading

Fig. 12 Plaxis 3D model for foundation with structure under dynamic loading

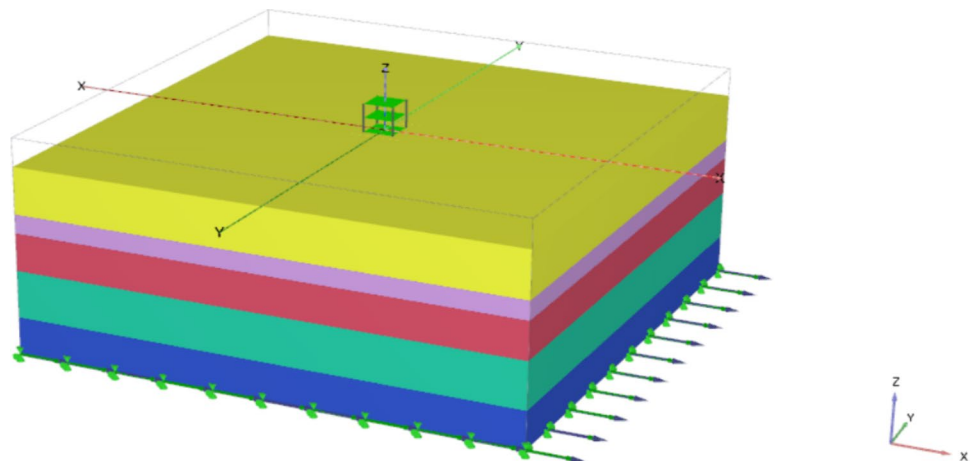


Fig. 13 Vertical settlement versus time plot at 1 m from Ground Surface for free field condition, foundation alone and foundation with structure under dynamic loading

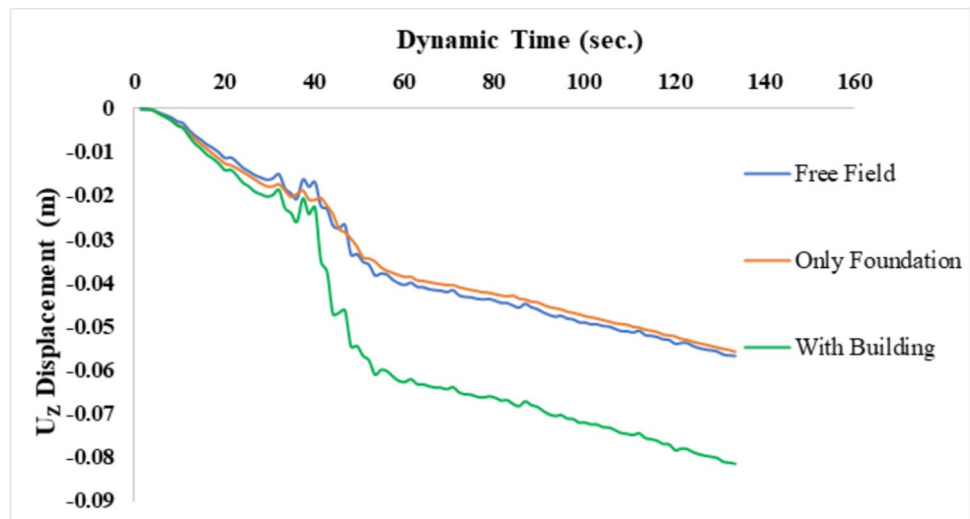
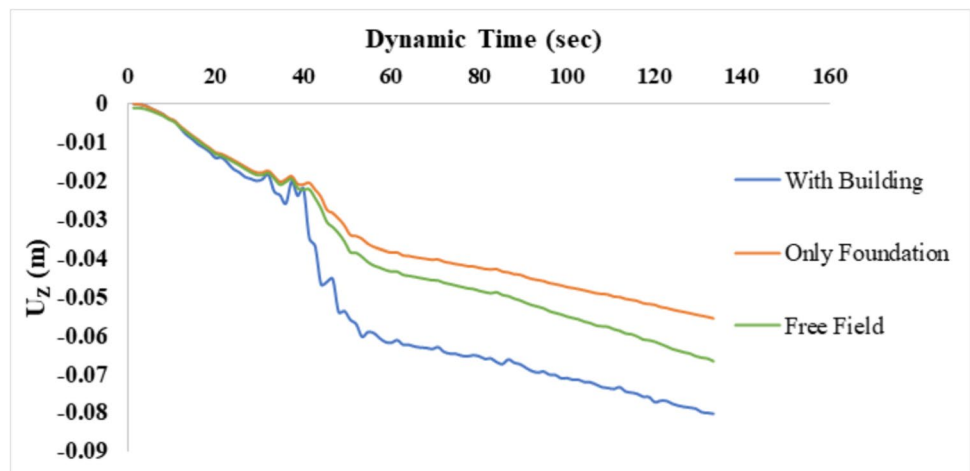


Fig. 14 Horizontal deformation versus time plot at ground surface for free field condition, foundation alone and foundation with structure under dynamic loading



bottom, a compliant base by Joyner and Chen [19] with a specified X-direction displacement of 1m was used.

Result and discussion

Static analysis

Two aspects have been considered for static analysis.

Case 1- foundation alone subjected to dynamic loading.

Case 2- foundation with structure subjected to dynamic loading.

Bearing capacity

In the research, a circular footing with a 1 m radius was evaluated for assessing soil bearing capacity, and an isolated footing with a predefined vertical downward

displacement of 0.5 m was examined. Figure 7 shows the model used for determining bearing capacity.

Figure 8 illustrates the load settlements curve used for determining bearing capacity. The settlement was measured at a depth of 1 m from the foundation's bottom. The double tangent approach determined the Bearing Capacity to be around 270 kN/m². According to IS 1904 (1986), a 75 mm settlement is permitted for a circular foundation built on clayey soil. About 208 kN/m² of bearing capacity was determined to correlate with 75 mm settlement. Therefore, the maximum allowable load for each footing was calculated to be 653 kN, which was larger than the load provided via each footing by the building i.e., 195 kN.

Settlement

In all scenarios, it was determined that the structures and foundations were safe and their settlement was within the

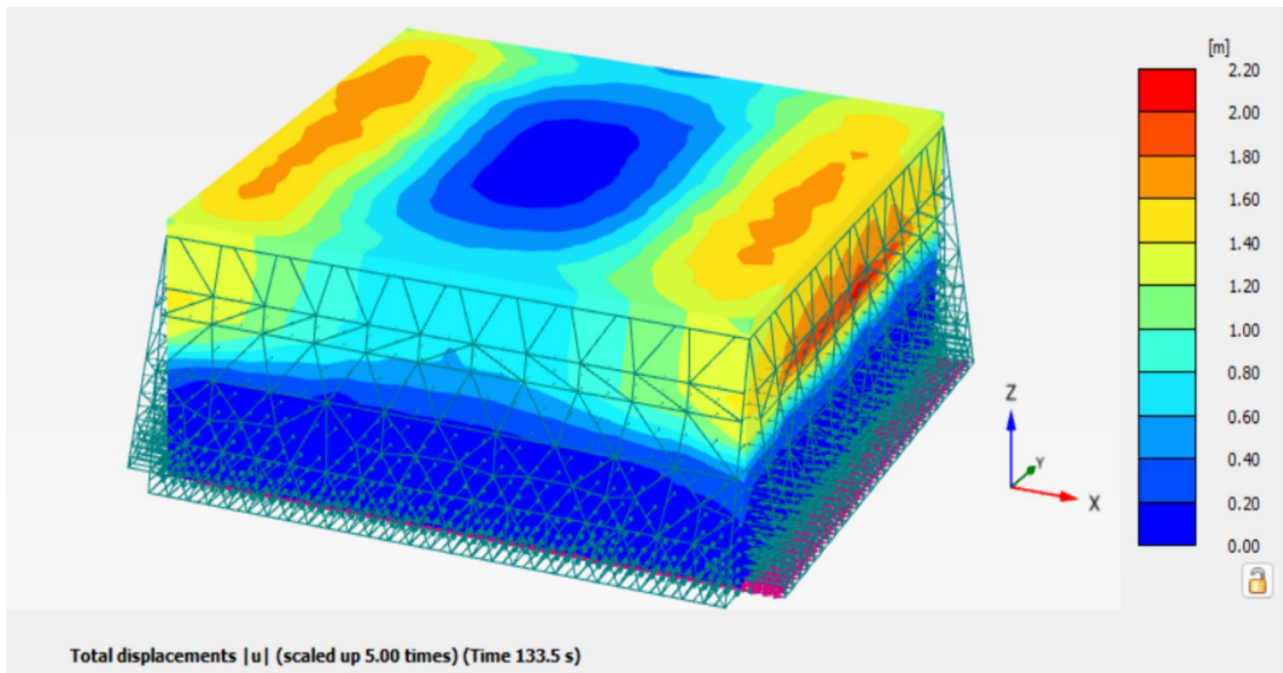


Fig. 15 Pressure bulb for foundation alone under dynamic loading

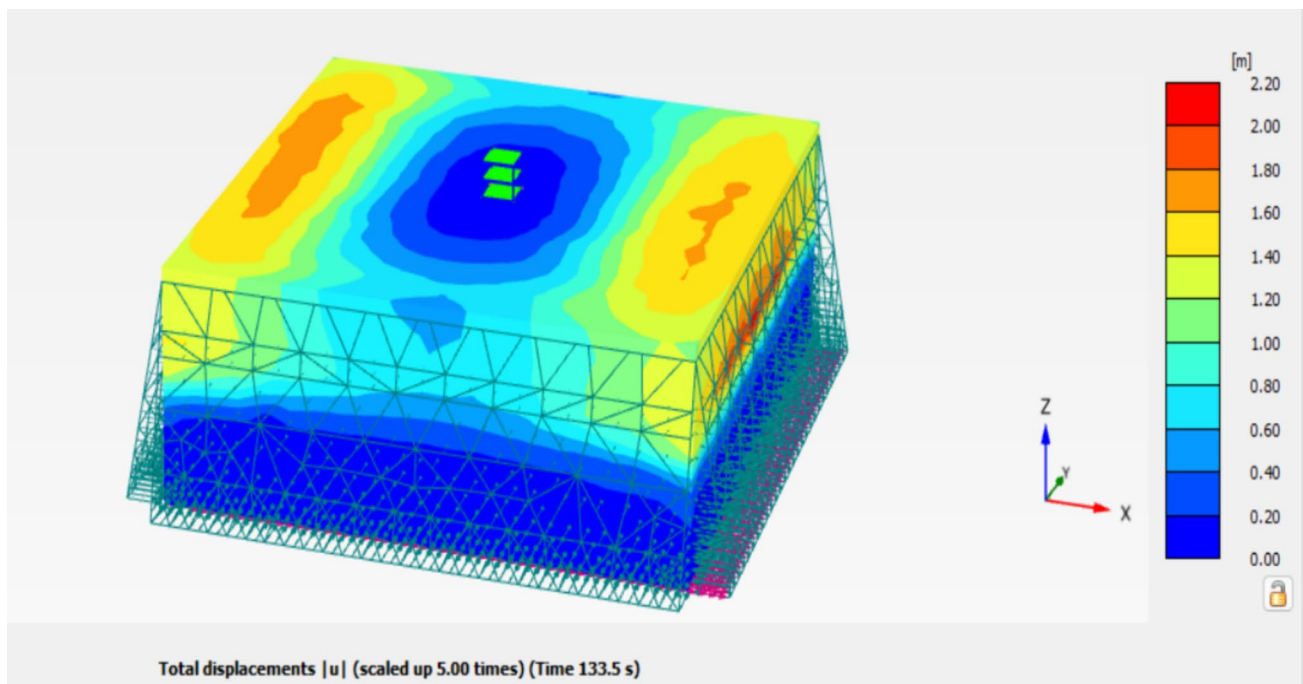


Fig. 16 Pressure bulb for foundation with structure under dynamic loading

Table 4 Settlement in dynamic case

Deformation (mm)	Free field	Only foundation	With building
Vertical	80	37.72	85.64
Horizontal	106	87.64	110

acceptable range. The horizontal and vertical settlement for both situations are shown in Table 3.

The degree of pressure was maximum under the foundation and reduced with depth, as shown in Fig. 9. The pressure bulb for the instance of a structure with a foundation

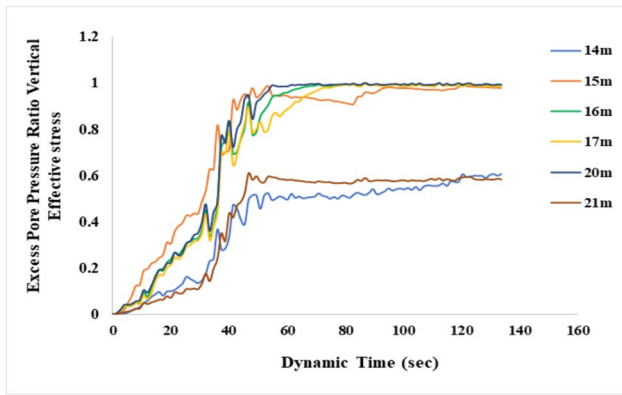


Fig. 17 R_u versus time plot for vertical effective stress for foundation with structure under dynamic loading

Fig. 18 R_u versus time for mean effective stress for foundation with structure under dynamic loading

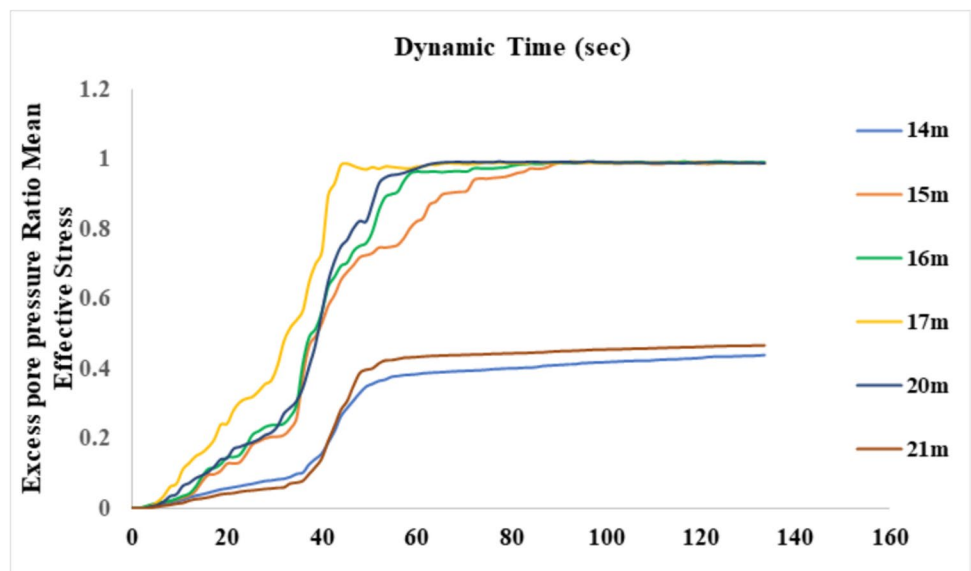
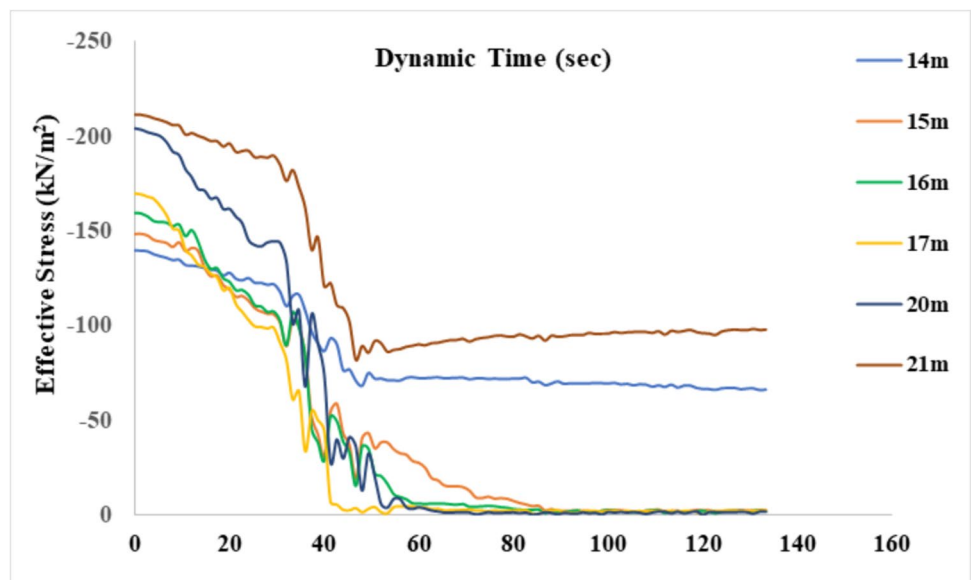


Fig. 19 Effective stress-time history for foundation with structure under dynamic loading



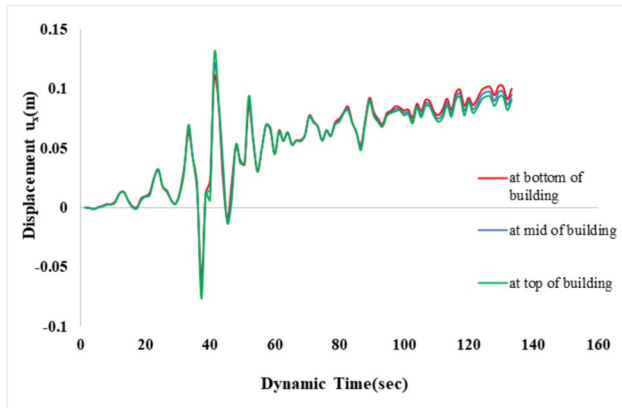
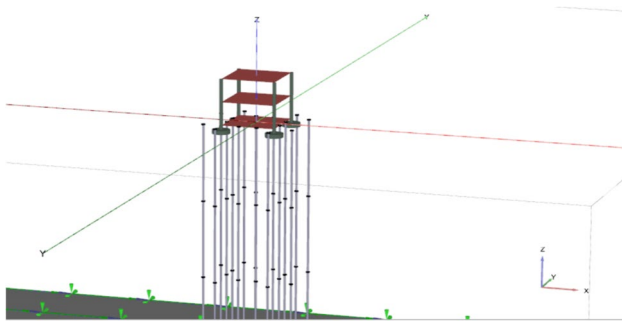
is shown in Fig. 10. The largest deformation was detected underneath and below the inner corner of the foundation, as shown in Fig. 10. Figure 10 further reveals that the pressure intensity extended laterally higher after structural load application.

Stress–strain characteristics

Shear strength is defined as the maximum shear stress that a material can endure. The shear strength versus shear strain plot was determined and shown in Fig. 11. The curve was developed for a circular footing with a 1 m radius and a 500 kN/m² load in the middle of the clay layer. Study

Table 5 Building deformation at different levels

	At bottom	At middle	At top
Horizontal (mm)	108	119	129
Vertical (mm)	81	82	82

**Fig. 20** Displacement versus time plot at a different building level foundation with structure under dynamic loading**Fig. 21** Plaxis 3D model for liquefaction mitigation using vertical drains

reveals that soil acts as normally consolidated clay. For a given stress value, it was observed that the strain in the xz -plane was much larger than the strain in the yz -plane.

Dynamic analysis

In Dynamic analysis, three scenarios have been considered (i.e., (i) Free Field (ii) Foundation Alone and (iii) Foundation with structure) for the research. Figure 12 depicts Plaxis 3D model of foundation with structure.

Settlement

In all three situations, vertical and horizontal deformations were observed, and settlement vs time plot were plotted at a depth of 1 m below the surface of the ground. The settlement in the vertical direction for each scenario is represented in Figs. 13 and 14. The maximum vertical settlement was reported to be larger in the scenario when building load is considered than in case of free field and only foundation is present. This is because during an earthquake settlement behaviour can be affected by the presence of a building or structure. The building's weight and dynamic response to ground motion can interact with the soil, leading to additional settlement.

Figures 15 and 16 depict the pressure bulb for the case 1 and case 3, respectively. From Figs. 15 and 16, it can be said that Case 3 experienced larger vertical and horizontal deformation than Case 1 and case 2. It can also be observed that the largest settlement developed near the extreme of the soil domain in the direction of seismic load impact. From Table 4, it is evident that the largest settlement was recorded in the case 3.

Excess pore pressure ratio

R_u , which is the EPP divided by the initial effective vertical stress at that depth, may be employed to determine the liquefaction potential. During liquefaction, the value of R_u approaches or surpasses 1. When R_u approaches or surpasses 1, it indicates that the buildup of excess pore pressure is significant relative to the initial effective stress. The R_u at various depths can be seen in Figs. 17 and 18 for Case 3. From Figs. 17 and 18, it can be derived that the R_u was largest at a depth of 20 m, and that at depths of 15 m, 16 m, 17 m, and 20 m, the value of R_u approaches 1, indicating complete liquefaction. Also, the graphs show that R_u and EPP converge towards 1 primarily within the sand layer, indicating liquefaction susceptibility. This trend highlights the significance of soil type in assessing liquefaction potential, with sands being notably prone to liquefaction-induced hazards.

Effective stress

At various depths, the effective stress of the layer of sand was computed. Figure 19 illustrates the fluctuation in vertical effective stress in the sand layer at various depths. The graphs demonstrate that as the effective stress approaches zero within the sand layer particularly highlighting the vulnerability of sands to liquefaction. At depths of 16 m, 18 m, and 20 m, the effective stress becomes zero, indicating full liquefaction. The graphs

Fig. 22 EPP ratio-time history at various depths

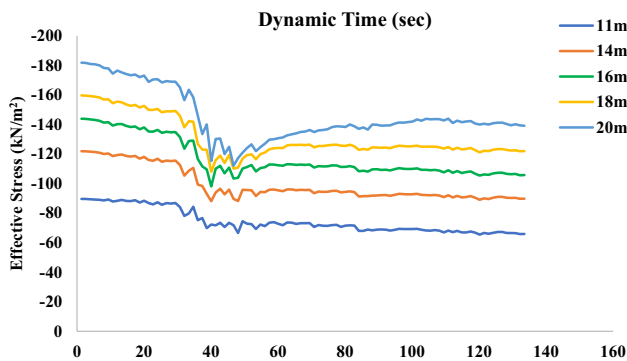
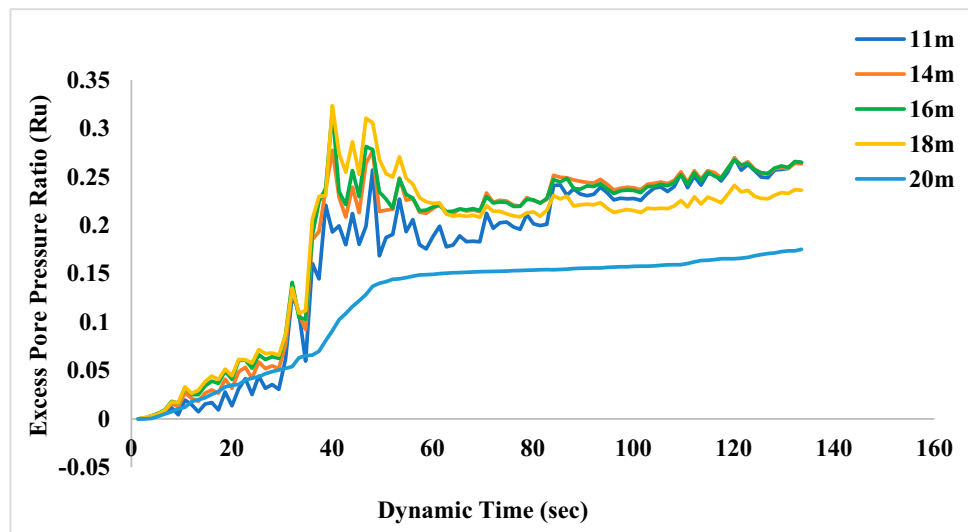


Fig. 23 Effective stress-time history at various depths

demonstrate that as the effective stress approaches zero within the sand layer,

Impact on building

Based on the findings, it was determined that vertical settlement at each level of the structure was practically identical. In the instance of horizontal displacement, the largest deformation was seen at the building's apex and the least at its base as seen in previous research (Tokimatsu et al. [19]). Table 5 represent the deformation on various levels of building.

Horizontal displacement–time history is shown in Fig. 20, and it was discovered that displacement was greatest at the building's top. The findings from Table 5 and Fig. 20 led to the conclusion that deformation increases

as distance from the ground increases, justifying the phenomenon known as seismic amplification.

Liquefaction mitigation using vertical drain

Polypropylene vertical drains with small cross-sectional area are used for the dissipation of EPP. Around the foundation, vertical drains were put in place to prevent liquefaction. Figure 21 depicts a model with vertical drains surrounding the foundation.

Utilizing a vertical drain relieves the excess pore pressure generated by dynamic loading, hence lowering the loss of effective stress. The impact was analysed, and it was discovered that the EPP ratio decreased with respect to dynamic time, hence increasing the effective stress, as seen in Figs. 22 and 23, respectively.

Conclusion

The research resulted in the following conclusion:

Under static conditions, deformations in both horizontal and vertical directions increased proportionally with the applied load. Analysis revealed that acceleration and deformation were most pronounced at the top of the building, diminishing with decreasing building height. Dynamic analysis indicated that vertical and horizontal deformations at the ground surface and beneath the foundation were maximized in the presence of buildings, with vertical deformation being less than horizontal deformation. The ratio of excess pore water pressure was highest in the presence of buildings, indicating an increased susceptibility to liquefaction. Furthermore, it was observed that there was a substantial reduction in effective stress and an increase in excess pore water pressure ratio with high-amplitude input signals. Vertical

drains were identified as an effective means to mitigate liquefaction by significantly reducing excess pore water pressure and increasing soil effective stress. However, further comprehensive investigations are warranted to determine the optimal orientation and efficacy of vertical drains for liquefaction mitigation strategies.

Limitations and future recommendations

This study has been done for the Bhuj (2001) earthquake, so it may be possible to get different results for another earthquake, so the results presented here are only for the Bhuj earthquake. This research does not account for the aftershock effect. It will have to be included in future analyses due to its importance in induced settlements and lateral spreading. More study is needed to be done to understand the influence of drainage for the mitigation of liquefaction. Also, more research is needed to compare prefabricated drains, stone columns, and sand drains for liquefaction mitigation. Keeping sustainability and judicious use of environmental resources in mind vertical drains which are composed of polypropylene and other toxic material are replaced by jute and other natural alternatives, then it will be commendable step toward sustainable development as this natural material are non-toxic and will not affect environment in negative way.

Author contributions All authors contributed equally to this work.

Funding The authors declare that no funds, grants, or other support were received during the preparation of this manuscript.

Data availability All the data used in this study are available from the corresponding author, upon reasonable request.

Declarations

Conflict of interest The authors declare that there is no conflict of interest.

References

- Tsegaye AB (2012) PLAXIS liquefaction model Rep. no. 1. PLAXIS Knowledge base., no. February 2010
- Abdullah A, Hazarika H (2016) Improvement of shallow foundation using non-liquefiable recycle materials. *Japn Geotech Soc Spec Publ* 2(54):1863–1867
- Abdullah A, Hazarika H, Yasufuku N, Ishikura R (2015) Numerical study on seismic response of quay wall reinforced with tire chips. In: *Computer methods and recent advances in geomechanics: proceedings of the 14th international conference of international association for computer methods and recent advances in geomechanics, 2014 (IACMAG 2014)*. Taylor & Francis Books Ltd., pp 1885–1889
- Ayoubi P, Pak A (2017) Liquefaction-induced settlement of shallow foundations on two-layered subsoil strata. *Soil Dyn Earthq Eng* 94:35–46
- Bauer E, Claussen M, Brovkin V, Huenerbein A (2003) Assessing climate forcings of the Earth system for the past millennium. *Geophys Res Lett*. <https://doi.org/10.1029/2002GL016639>
- Bouckovalas GD, Papadimitriou AG, Niarchos DG, Tsiapas YZ (2011) Sand fabric evolution effects on drain design for liquefaction mitigation. *Soil Dyn Earthq Eng* 31(10):1426–1439
- Bray JD, and Dashti S (2010) Liquefaction-induced movements of buildings with shallow foundations
- Dash SR, Govindaraju L, Bhattacharya S (2009) A case study of damages of the Kandla Port and customs office tower supported on a mat–pile foundation in liquefied soils under the 2001 Bhuj earthquake. *Soil Dyn Earthq Eng* 29(2):333–346
- Dashti S, Bray JD, Pestana JM, Riemer M, Wilson D (2010) Centrifuge testing to evaluate and mitigate liquefaction-induced building settlement mechanisms. *J Geotech Geoenviron Eng* 136(7):918–929
- Fasano G, De Sarno D, Bilotta E, Flora A (2019) Design of horizontal drains for the mitigation of liquefaction risk. *Soils Found* 59(5):1537–1551
- Forcellini D (2020) The role of the water level in the assessment of seismic vulnerability for the 23 november 1980 Irpinia-Basilicata earthquake. *Geosciences* 10(6):229
- Forcellini D (2021) Analytical fragility curves of shallow-founded structures subjected to soil-structure interaction (SSI) effects. *Soil Dyn Earthq Eng* 141:106487
- García-Torres S, Madabhushi GSP (2019) Performance of vertical drains in liquefaction mitigation under structures. *Bull Earthq Eng* 17:5849–5866
- Hanindya KA, Makrup L, Paulus R (2023) Deterministic seismic hazard analysis to determine liquefaction potential due to earthquake. *Civil Eng J* 9(5):1203–1216
- Harianto T, Muhiddin AB, Arsyad A (2023) Soil reinforcement model test using timber pile at liquefaction area. *Civil Eng J* 9(6):1509–1521
- Hayden CP (2014) Liquefaction-induced building performance and near-fault ground motions. University of California, Berkeley
- I.S. 1904 (1986) Code of practice for design and construction of foundations in soils: general requirements. Bureau Indian Stand, New Delhi
- Iyengar RN, Kanth SR (2006) Strong ground motion estimation during the Kutch, India earthquake. *Pure Appl Geophys* 163:153–173
- Joyner WB, Chen AT (1975) Calculation of nonlinear ground response in earthquakes. *Bull Seismol Soc Am* 65(5):1315–1336
- Kamao S, Takezawa M, Yamada K, Jinno S, Shinoda T, Fukazawa E (2014) A study of earthquake-caused liquefaction: the case of Urayasu City. *Earthq Soil Interact* 133:149–161
- Katayama T (2004). Earthquake disaster risk mitigation before and after the 1995 Kobe earthquake. In *13th world conference on earthquake engineering*, Vancouver
- Kayal JR, Zhao D, Mishra OP, De R, Singh OP (2002) The 2001 Bhuj earthquake: tomographic evidence for fluids at the hypocenter and its implications for rupture nucleation. *Geophys Res Lett* 29(24):1–5
- Komolafe OO, Balogun IO, Abiodun YO (2021) Comparison of square and circular isolated pad foundations in cohesionless soils. *Arid Zone J Eng Technol Environ* 17(2):197–210
- Kramer SL (1996) *Geotechnical earthquake engineering*. Pearson Education, India
- Li B, Li X (2023) Study on the test error of silt dynamic characteristic and its influence on the peak ground acceleration. *HighTech Innov J* 4(1):65–74

26. Liu L, Dobry R (1997) Seismic response of shallow foundation on liquefiable sand. *J Geotech Geo Environ Eng* 123(6):557–567
27. Lysmer J, Kuhlemeyer RL (1969) Finite dynamic model for infinite media. *J Eng Mech Div* 95(4):859–877
28. Waheed MQ, Asmael NM (2019) Study simulation of shallow foundation behavior using different finite element models. *J Adv Civ Eng Pract Res* 8(1):4–1
29. Marques ASPS, Coelho PALF, Cilingir U, Haigh SK, and Madabhushi G (2012) Earthquake-induced liquefaction effects on a shallow foundation. In: WCEE conference 2012
30. Mehrzad B, Jafarian Y, Lee CJ, Haddad AH (2018) Centrifuge study into the effect of liquefaction extent on permanent settlement and seismic response of shallow foundations. *Soils Found* 58(1):228–240
31. Onur MI, Tuncan M, Tuncan A (2016) Determination of earthquake effects on sandy soils for the city of Eskisehir, Turkey. *Disaster Sci Eng* 2(2):36–39
32. Rollins KM, Seed HB (1990) Influence of buildings on potential liquefaction damage. *J Geotech Eng* 116(2):165–185
33. Rollins KM, Goughnour RR, Anderson JKS, and Wade SF (2004) Liquefaction hazard mitigation by prefabricated vertical drains
34. Rajarathnam S, Renu MS, Santhakumar AR, Premalatha K (2014) Liquefaction hazard assessment and building foundation safety for Chennai city, India. *Disaster Adv* 7(11):1–13
35. Seed HB, Booker JR (1977) Stabilization of potentially liquefiable sand deposits using gravel drains. *J Geotech Eng Div* 103(7):757–768
36. Singh M, Maheshwari BK (2022) Effect of liquefaction on behavior of strip footings on sands in Roorkee. In: Satyanarayana Reddy CNV, Krishna AM, Satyam N (eds.), *Dynamics of soil and modelling of geotechnical problems*. Lecture notes in civil engineering, vol 186. Springer. https://doi.org/10.1007/978-981-16-5605-7_27
37. Sitharam TG, Govindaraju L (2004) Geotechnical aspects and ground response studies in Bhuj earthquake, India. *Geotech Geol Eng* 22:439–455
38. Taiebat M, Shahir H, Pak A (2007) Study of pore pressure variation during liquefaction using two constitutive models for sand. *Soil Dyn Earthq Eng* 27(1):60–72
39. Tokimatsu K, Hino K, Suzuki H, Ohno K, Tamura S, Suzuki Y (2019) Liquefaction-induced settlement and tilting of buildings with shallow foundations based on field and laboratory observation. *Soil Dyn Earthq Eng* 124:268–279
40. Viladkar MN, Singh M, Samadhiya NK (2019) Liquefaction analysis of metro underground tunnels. *Earthquake geotechnical engineering for protection and development of environment and constructions*. CRC Press, Boca Raton, pp 5539–5546
41. Wakamatsu K, and Numata A (2004) Effect of liquefaction susceptibility on building damage during the 1995 Kobe earthquake. In: *Proceedings of 13th WCEE*, paper (377)
42. Yasui M (1992) Settlement and inclination of reinforced concrete buildings in Dagupan City due to liquefaction during the 1990 Philippine earthquake. In: *Earthquake engineering, tenth world conference*

Springer Nature or its licensor (e.g. a society or other partner) holds exclusive rights to this article under a publishing agreement with the author(s) or other rightsholder(s); author self-archiving of the accepted manuscript version of this article is solely governed by the terms of such publishing agreement and applicable law.